

# The Structure of a Trimolecular Liquid: *tert*-Butyl Alcohol:Cyclohexene:Water

D. T. Bowron<sup>\*,†</sup> and S. Díaz Moreno<sup>‡</sup>

ISIS Facility, CLRC Rutherford Appleton Laboratory, Chilton, Didcot, OX11 0QX, United Kingdom, and  
Diamond Light Source Ltd., Rutherford Appleton Laboratory, Chilton, Didcot, OX11 0QX, United Kingdom

Received: June 1, 2005; In Final Form: July 6, 2005

The structure of the trimolecular liquid mixture of 2:6:1 cyclohexene, *tert*-butyl alcohol, and water has been investigated using hydrogen/deuterium substitution neutron scattering techniques, and a three-dimensional structural model refined to be consistent with the experimental data has been built using the technique of Empirical Potential Structure Refinement. The model shows a well-mixed solution of the three molecular components where the competing interactions between the nonpolar cyclohexene and polar water molecules are balanced in the solution leading to largely pure-alcohol-like interactions between the *tert*-butyl alcohol molecules. Cyclohexene molecules favor direct solvation by alcohol methyl groups while water molecules are accommodated, dispersed throughout the solution, via hydrogen bonding interactions with the alcohol molecule hydroxyl groups. Rare occurrences of direct cyclohexene–water interactions are of the classic hydrophobic hydration type and no evidence is found for microscopic heterogeneity in the trimolecular mixture in contrast to the general findings for binary alcohol–water solutions.

## I. Introduction

Alcohols are often and widely chosen as a good solvent medium in which to perform chemical reactions because their amphiphilic nature is well suited to the accommodation of both polar and nonpolar solute species in solution. In this role the alcohol can act as a reaction facilitating medium that enables otherwise immiscible reaction components to be brought into sufficiently close proximity for them to interact. Fundamentally underlying the remarkable property of alcohols to solvate a wide range of solute species are the complex range of intermolecular interactions that these solutions support. Recent advances in experimental structure determination of liquids by neutron scattering techniques are increasingly allowing us to look in great detail at the nature of these intermolecular interactions in both a chemically specific and molecular orientation sensitive manner.<sup>1</sup> Central to the establishment of neutron scattering techniques as a particularly powerful means to investigate the structure of liquids has been the development of isotopic substitution methods that allow the labeling of chemically specific atomic sites on a system's constituent atoms and molecules.<sup>2</sup> In particular, for aqueous and organic liquids, the variant of the technique based on neutron diffraction with hydrogen/deuterium substitution has proven exceptionally useful.<sup>3</sup> To date, the majority of investigations using these methods have focused attention on the structure of pure molecular liquids or binary mixtures thereof, though nothing fundamental inhibits the extension of the technique to ternary or more complex systems. The information derived by such methods has proven invaluable for assisting us to develop our understanding of the fine balance between the various interactions that occur between nonpolar and polar entities in solution and for enhancing our insight into how hydrogen bonding interactions can play a key role in shaping the available molecular environments.

*tert*-Butyl alcohol is a typical monohydric alcohol that is widely used as a solvent medium and is known to be the largest alcohol of this type to remain fully miscible in water at all concentrations.<sup>4</sup> Increasing the number of nonpolar groups enhances the hydrophobic nature of the series at the expense of the aqueous solubility provided by the single polar hydroxyl group. This alcohol therefore provides an ideal system in which a fine balance between polar and nonpolar molecular interactions can be studied as well as the response of this balance to the addition of polar or nonpolar solute species. Structural investigations of the pure alcohol<sup>5,6</sup> have highlighted the details of nonpolar and polar molecular interactions and the experimental results show that though intermolecular hydrogen bonding is important in the system, direct nonpolar group to nonpolar group interactions play a more significant role in the solution structure than classical models would predict. Addition of water to this system in various quantities, i.e., a polar solute or solvent depending on whether the alcohol or water is the dominant mixture component, has been shown to markedly affect the nature of the alcohol interactions.<sup>7,8</sup> Regardless of concentration the addition of water to the alcohol disrupts direct hydrogen bonding interactions between alcohol molecules, substituting hydrogen bonds between the water molecules themselves and the alcohol hydroxyl group. This change in the polar interactions between the alcohol molecules subsequently drives a preference for direct interactions between alcohol nonpolar methyl groups and can be considered a classic example of the hydrophobic interaction.<sup>9</sup> Binary solutions of *tert*-butyl alcohol and water display characteristic features of microscopic segregation of the two solution components that have been observed in several other monohydric alcohol–water systems and that seem to be a ubiquitous property of the mixtures.<sup>10–12</sup>

To go further and begin to understand the structural foundation for the alcohols' ability to be a useful reaction facilitating medium accommodating both nonpolar and polar species in solution it is necessary to investigate the addition of a nonpolar molecular species as a cosolute with a polar molecule such as

\* Address correspondence to this author. E-mail: d.t.bowron@rl.ac.uk.  
Phone: +44 (0) 1235-446-397. Fax: +44 (0) 1235-445-720

<sup>†</sup> ISIS Facility, CLRC Rutherford Appleton Laboratory.

<sup>‡</sup> Diamond Light Source Ltd.

water. A model example based on the *tert*-butyl alcohol–water system and that has practical application to a real reaction system is the addition of a nonpolar alkene as a cosolute. This combination of alcohol, water, and alkene is a typical molecular mixture found in the important chemical process used to produce cis-diols by the cis-hydroxylation of alkenes by osmium tetroxide.<sup>13</sup> Here we utilize the neutron scattering with H/D substitution technique to investigate the detailed structure of a trimolecular liquid of 2:6:1 cyclohexene, *tert*-butyl alcohol, and water. The alcohol–water stoichiometry was selected to mirror the composition of the organic phase solvent widely used in osmium tetroxide based dihydroxylation reactions, while the quantity of alkene was simply chosen to allow good structural contrast for the neutron scattering experiment. The aim is to investigate how the combined addition of the nonpolar cyclic alkene and polar water molecules to this monohydric alcohol perturb the dominant interactions between the molecules of the bulk solution component, and furthermore investigate how each of the minor components is structurally accommodated in the mixture.

## II. Theory

The total structure factor,  $F(Q)$ , measured for a liquid or glass by a neutron diffraction experiment allows us to determine a function called the total atomic pair distribution function  $g(r)$ . This function, obtained by a Fourier transform of the  $F(Q)$ , represents the interatomic distance correlations between all pairs of atoms within the solution.<sup>14</sup>

$$F(Q) = 4\pi\rho \int_0^\infty r^2 [g(r) - 1] \frac{(\sin(Qr))}{Qr} dr$$

$$g(r) - 1 = \frac{1}{(2\pi)^3 \rho} \int_0^\infty 4\pi Q^2 F(Q) \frac{(\sin(Qr))}{Qr} dQ \quad (1)$$

$\rho$  is the atomic density of the system,  $Q = (4\pi/\lambda) \sin(\theta)$  is the magnitude of the momentum transfer vector of the scattered neutrons, and  $2\theta$  is the scattering angle.

A neutron scattering experiment on a single sample with known atomic and isotopic composition will produce one total structure factor  $F(Q)$ . Often this can be a complex function to interpret in a many component system, but by performing a series of measurements on isotopically distinct samples, and assuming all other factors between each sample are negligibly changed, i.e., precise composition and structure, it becomes possible to simplify the challenge. A series of isotope labeled scattering data can be probed to extract more detailed information about specific site–site partial structure factors and obtain chemically specific insight into the correlations between the structural units that have been labeled. This is the basis of the technique of neutron diffraction with isotopic substitution pioneered by Enderby and Neilson.<sup>2</sup> The application of this method to binary molecular mixtures is now well established and details are readily available in the literature, see, for example, the review by Finney and Soper.<sup>3</sup>

## III. Experimental Section

To extract structural information on the trimolecular mixture of cyclohexene, *tert*-butyl alcohol, and water, a series of nine neutron diffraction experiments were performed using hydrogen/deuterium labeling techniques to highlight intermolecular correlations between the three mixture components. The nine solutions measured were the following: (1)  $C_6H_{10}$ ,  $C_4D_9OD$ ,  $D_2O$ ; (2)  $C_6H_{10} + C_6D_{10}$  in a 1:1 ratio,  $C_4D_9OD$ ,  $D_2O$ ; (3)  $C_6D_{10}$ ,

**TABLE 1: Neutron Scattering Lengths Relevant to Cyclohexene, *tert*-Butyl Alcohol, Water Solutions**

element/ isotope	scattering length (fm)
C	6.646
O	5.803
H	−3.739
D	6.671

$C_4D_9OD$ ,  $D_2O$ ; (4)  $C_6D_{10}$ ,  $C_4H_9OD$ ,  $D_2O$ ; (5)  $C_6D_{10}$ ,  $C_4H_9OD + C_4D_9OD$  in a 1:1 ratio,  $D_2O$ ; (6)  $C_6H_{10}$ ,  $C_4D_9OH$ ,  $H_2O$ ; (7)  $C_6D_{10}$ ,  $C_4H_9OH$ ,  $H_2O$ ; (8)  $C_6D_{10}$ ,  $C_4H_9OH + C_4D_9OD$  in a 1:1 ratio,  $H_2O + D_2O$  in a 1:1 ratio; and (9)  $C_6D_{10}$ ,  $C_4D_9OH$ ,  $H_2O$

Each solution was prepared to a molecular stoichiometric ratio for cyclohexene:*tert*-butyl alcohol:water of 2:6:1 and the solutions that involve two isotopically distinct forms of one or more of the molecular components were made to maintain a 1:1 mixture between the two isotopic forms. The atomic density of each sample was  $\sim 0.1$  atoms  $\text{\AA}^{-3}$ . The scattering lengths used for the elements and isotopes relevant to this analysis are given in Table 1.

Measurements of the neutron scattering from each solution were performed on the Small Angle Neutron Diffractometer for Amorphous and Liquid Samples (SANDALS) at the ISIS pulsed neutron facility, Rutherford Appleton Laboratory, UK. Each sample was contained in flat  $Ti_{0.68}Zr_{0.32}$  alloy cells of internal dimensions 35 mm (width)  $\times$  35 mm (height)  $\times$  1 mm (thickness) and mounted on the instrument's automatic sample changer to control the sample temperature at  $25 \pm 1$  °C. The alloy composition of the cell was selected such that the sample container made zero contribution to the coherent scattering cross section of the measured sample. The thickness of the TiZr cell walls was 1 mm for each surface bounding the sample volume.

The scattering data were collected over scattering angles ( $2\theta$ ) between 3° and 40° and analyzed using neutron wavelengths in the range from  $\lambda = 0.05$  to 3.5  $\text{\AA}$  over a corresponding  $Q$ -range for each data set ranging from 0.15 to 50  $\text{\AA}^{-1}$ . For each sample the data were normalized to the scattering from a vanadium standard and corrected for background scattering, sample absorption, and multiple scattering using the Gudrun package developed by Soper<sup>15</sup> that evolved from the widely used Atlas package.<sup>16</sup> The single atom scattering and inelasticity corrections were performed by the method outlined in Soper and Luzar<sup>17</sup> and the end result of these processing steps is the total structure factor,  $F(Q)$ .

The application of first and second order difference neutron diffraction techniques<sup>3</sup> gives us direct access to many of the key intermolecular and interatomic interactions that define the solution structure and hence its physicochemical properties; in particular, (a) solutions 1, 2, and 3 give us direct access to the intermolecular correlations between the hydrogen sites on the cyclohexene rings, (b) solutions 3, 4, and 5 provide access to the alcohol–alcohol structural correlations from the viewpoint of the methyl hydrogen sites on the alcohol molecules, (c) solutions 3, 7, and 8 give structural information relating to the correlations between the alcohol and water hydrogen sites in the trimolecular liquid, and (d) solutions 3 and 9, or 1 and 6, provide access to alcohol hydroxyl hydrogen and water hydrogen centered information.

To maximize the amount of structural information that could be obtained from the measured scattering data, the technique of Empirical Potential Structure Refinement (EPSR)<sup>18–20</sup> has been utilized to derive an ensemble of structural models that can simultaneously satisfy all nine measured structure factors. These structural models can then be subsequently interrogated

**TABLE 2: Lennard-Jones, Charge, and Atomic Mass Parameters Used for the Reference Potentials that Seed the Empirical Potential Structure Refinement Model of the Cyclohexene + *tert*-Butyl Alcohol + Water Solution.**

atom type	$\epsilon$ , kJ mole <sup>-1</sup>	$\sigma$ , Å	$M$ , amu	$q$ , e
CC	0.299	3.28	12	0.265
C	0.299	3.28	12	0.000
M	0.189	2.58	1	0.000
O	0.712	3.07	16	-0.700
H	0.000	1.35	1	0.435
OW	0.650	3.16	16	-0.8476
HW	0.000	0.00	2	0.4238
C2	0.299	3.21	12	0.000
C3	0.299	3.21	12	0.000
H2	0.189	2.58	2	0.000
H3	0.189	2.58	2	0.000

to extract structural quantities of interest such as atomic partial pair distribution functions, coordination numbers, and molecular orientational correlation functions. Throughout this work the following labels have been assigned to the distinguishable atomic sites on each of the three molecular species (1) for *tert*-butyl alcohol, CC, C, M, O, and H correspond respectively to central carbon, methyl group carbon, methyl group hydrogen, hydroxyl group oxygen, and hydroxyl group hydrogen, (2) for water, OW and HW correspond to the oxygen and hydrogen sites, respectively, and (3) for cyclohexene, C2, C3, H2, and H3 respectively refer to carbon atoms involved in the C=C double bond, carbon atoms not involved in double bonding, hydrogen bonded to a double bonded carbon, and hydrogen bonded to a nondouble bonded carbon. The Lennard-Jones and charge parameters used to seed the structure refinement are given in Table 2.

#### IV. Structure Refinement

The EPSR method is based upon classical Monte Carlo simulation methods for molecular liquids.<sup>21</sup> However, in contrast to conventional Monte Carlo modeling, the evolution of the model system is linked to experimentally measured structure factor data. The linkage between model and data is achieved by perturbations applied to the set of atomic reference potentials driving the simulation by an empirical potential of mean force (eq 2). These perturbations can be derived from the experimentally determined radial distribution functions, or equally from the measured structure factors.

$$\psi_{\alpha}\beta(r) = -kT \ln[g_{\alpha}\beta(r)] \quad (2)$$

The method was in part developed to address the central problem that in most cases the number of isotopic variation experiments that can be performed on a multicomponent system is insufficient to allow the direct inversion of the scattering matrix to a complete structural solution. The details of the most current implementation of this technique, as utilized in this study, can be found in ref 22.

#### V. Results

**A. Model Fit to Experimental Data.** Figure 1 shows the experimental total structure factors for each of the nine isotopic solutions measured, along with the EPSR fit and fit residual obtained during the structure refinement procedure. It is worth noting that the fitting results presented, simultaneously satisfy the nine independent data sets with a single structural model. In general the fits are good across the  $Q$ -range, though for the data corresponding to the samples containing the largest quantity of light hydrogen, there remains a small rise in the fit residual at low  $Q$ . As this misfit occurs most significantly in the light

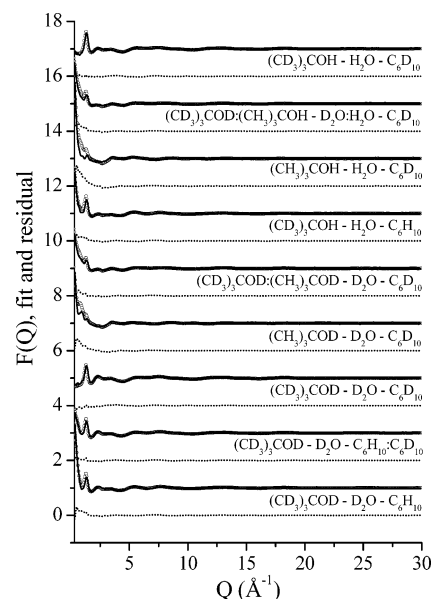


**Figure 1.** Experimental  $F(Q)$  data (circles), EPSR fits (solid line), and fit residuals (broken line) to nine isotopically distinct solutions of cyclohexene, *tert*-butyl alcohol, and water in a molecular ratio of 2:6:1.

hydrogen samples it is probably due to a data analysis artifact resulting from the imperfect correction of inelastic scattering effects achieved in the data preprocessing. The low-frequency components of this misfit, however, mean that it makes no significant contribution to the structure refinement over the interatomic and intermolecular length scales of interest here.

**B. Molecular Centers Distribution Functions.** Among the most informative pair distribution function for a molecular system is the molecular centers distribution function. This illustrates the structural correlations between molecule types averaged over all orientations of each molecule. Such functions are generally not directly accessible to experimental determination but are readily computed functions in computer simulations. The hybrid nature of the EPSR technique is thus ideally suited to the estimation of these complex structure functions. For the *tert*-butyl alcohol molecule a good approximation to its molecular center is the central carbon atom, for the water molecule the oxygen atom serves this role, and for the cyclohexene molecule it is useful to think in terms of a pseudo atom position derived as the mean position of the carbon atoms that make up the six-member ring. In these terms, Figure 2 shows the molecular centers functions that define the basis of the intermolecular correlations in the trimolecular solution. The persistence of strong oscillatory features extending to more than 15 Å radial distance from the center of the dominant solution components, *tert*-butyl alcohol and cyclohexene, show that considerable local ordering effects for the larger molecules occur in this system. In contrast the like-molecule water–water interactions appear to be dominated by short-range correlations on length scales from 2.5 to 6 Å.

The first two features in the *tert*-butyl alcohol–*tert*-butyl alcohol centers function (Figure 2A) relate to direct contact interactions between alcohol molecules. The first sharp peak centered at  $\sim 4.6$  Å has been shown in earlier studies of the pure alcohol<sup>5,6</sup> to relate to alcohol–alcohol interactions via interhydroxyl group hydrogen bonding. The second peak at  $\sim 5.8$  Å was similarly shown to relate to alcohol interactions by nonpolar group to nonpolar group contacts. Integrating beneath these features to obtain an estimate of the alcohol–alcohol coordination numbers shows that each alcohol molecule is



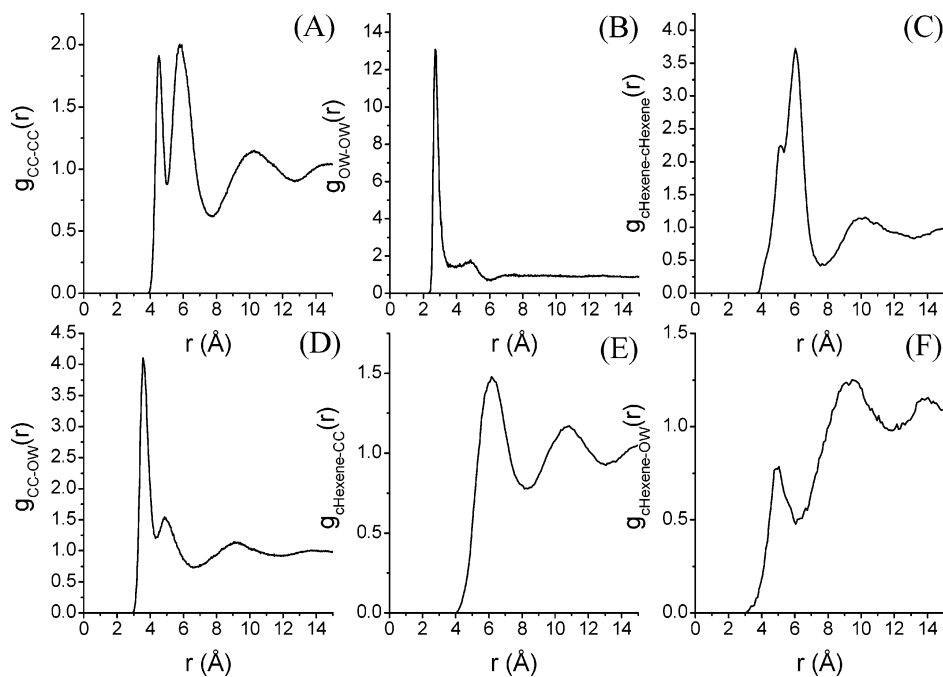


**Figure 2.** Molecular center distribution functions determined from the EPSR refinement for (A) *tert*-butyl alcohol–*tert*-butyl alcohol (CC–CC), (B) water–water (OW–OW), (C) cyclohexene–cyclohexene (cHexene–cHexene), (D) *tert*-butyl alcohol–water (CC–OW), (E) cyclohexene–*tert*-butyl alcohol (cHexene–CC), and (F) cyclohexene–water (cHexene–OW). The center of the *tert*-butyl alcohol molecule is defined as the position of the molecule's central carbon atom CC, the center of the water molecule is defined as the position of the water oxygen atom OW, and the center of the cyclohexene molecule is defined as the average position of the carbon atoms in the six-membered ring.

involved on average with  $1.4 \pm 0.1$  other alcohol molecules via hydrogen bonding interactions and with  $7.9 \pm 0.3$  alcohol molecules through nonpolar group interactions. These compare with values of  $1.2 \pm 0.2$  and  $9.6 \pm 0.5$  determined for a pure solution of *tert*-butyl alcohol.

In contrast to the similarities found with the pure liquid case for the alcohol–alcohol molecular centers function, the features in the water–water centers function (Figure 2B) are quite different from those found in pure bulk water.<sup>23</sup> In this trimolecular solution, water is only present at the 1 in 9 level by molecular ratio, and at lower levels by occupied volume. There is thus insufficient water in the system to produce extended bulk water-like intermolecular correlations. The main peak of the water–water centers function does, however, occur at the standard distance of  $\sim 2.7$  Å consistent with intermolecular hydrogen bonding, though its integrated area shows that on average each water molecule is in contact with only  $0.5 \pm 0.1$  other water molecules in the range from 2.3 to 3.8 Å. On average each water molecule will find  $1.2 \pm 0.2$  water molecules within a radius of 5.9 Å.

The molecular centers function for cyclohexene–cyclohexene correlations (Figure 2C) has been generated based on the distribution of ring centers. The function is peaked at a distance of  $\sim 6$  Å and integration of this function shows that each cyclohexene molecule will have  $\sim 4.2$  cyclohexene neighbors within a radius of 7.5 Å of its ring center. This can be compared with estimated coordination numbers for pure liquids of six-member cyclic molecules, cyclohexane and benzene, of  $\sim 13$ .<sup>24</sup>

The cross-correlations between the centers of different molecule types tell us about the solvation of each species by the other molecules in the mixture. Figure 2D shows the *tert*-butyl alcohol–water centers correlations function, which is equally the water–*tert*-butyl alcohol function. The integral of the first sharp peak at  $\sim 3.6$  Å, a distance that corresponds to a separation of alcohol and water molecule centers consistent with water molecules in the vicinity of the hydroxyl group of the

alcohol,<sup>25</sup> tells us that each alcohol has  $0.4 \pm 0.04$  water molecule centers in this range, or that each water molecule has  $2.4 \pm 0.2$  alcohol centers at that approximate distance. The second peak in the alcohol–water centers function at  $\sim 4.8$  Å corresponds to water molecules involved in the hydration of the nonpolar methyl group regions of the alcohol molecule. The coordination number calculated on integration of this feature tells us that each alcohol molecule will have on average  $0.7 \pm 0.05$  water molecules in its hydrophobic hydration shell, or alternatively that each water molecule finding itself in the nonpolar hydration region around an alcohol molecule will have  $4.4 \pm 0.3$  alcohol molecule neighbors coordinating via this kind of hydrophobic interaction.

Figure 2E shows the cyclohexene–*tert*-butyl alcohol molecule centers function that displays clear oscillatory structure across the entire displayed range out to 15 Å radius. These strong oscillations in this unlike molecular centers function suggest considerable correlation in the packing of these two large molecular species in the mixture. This is perhaps to be expected as both the cyclohexene and *tert*-butyl alcohol molecules have a similar size, as illustrated by the similar position,  $\sim 6$  Å, of the direct molecular contact features in the like molecule centers functions, Figure 2A,C. The similar position of the direct contact feature displayed in the cyclohexene–*tert*-butyl alcohol cross correlation confirms this finding. On integration of the first peak in this centers function, we determine that on average each cyclohexene molecule has  $\sim 9.5$  *tert*-butyl alcohol neighbors, and each *tert*-butyl alcohol molecule has  $\sim 3.2$  cyclohexene molecule neighbors. These relative numbers are consistent with the molecular stoichiometry of the solution.

Figure 2F shows the final unlike-species molecular centers function required to characterize the three-component system, i.e., showing the correlations between cyclohexene and water. The function has two main features, the first at  $\sim 5.0$  Å and the second at  $\sim 9.4$  Å, that can be assigned to direct contact interactions between water and cyclohexene and buffered

**TABLE 3: Coordination Numbers Calculated from Integration of Features in the Indicated Partial and Molecular Centers Distribution Functions**

correlation	density	$R_{\min}$	$R_{\max}$	coordination no.
CC–CC	0.0048	4.0	5.0	$1.4 \pm 0.1$
		5.0	7.7	$7.9 \pm 0.3$
		4.0	7.7	$9.3 \pm 0.3$
OW–OW	0.0008	2.3	3.8	$0.5 \pm 0.1$
		3.8	5.9	$0.6 \pm 0.2$
		2.3	5.9	$1.2 \pm 0.2$
CC–OW	0.0008	3.0	4.4	$0.4 \pm 0.04$
		4.4	6.6	$0.7 \pm 0.05$
OW–CC	0.0048	3.0	4.4	$2.4 \pm 0.2$
		4.4	6.6	$4.4 \pm 0.3$
O–O	0.0048	2.3	3.8	$1.6 \pm 0.1$
		3.8	5.9	$2.0 \pm 0.1$
O–H	0.0048	1.3	2.5	$0.7 \pm 0.05$
		2.5	4.8	$1.8 \pm 0.1$
H–H	0.0048	1.5	3.7	$1.7 \pm 0.1$
		3.7	5.6	$1.7 \pm 0.1$
O–OW	0.0008	2.3	3.8	$0.4 \pm 0.04$
		3.8	6.3	$0.6 \pm 0.05$
OW–O	0.0048	2.3	3.8	$2.3 \pm 0.2$
		3.8	6.3	$3.7 \pm 0.3$
O–HW	0.0016	1.3	2.4	$0.2 \pm 0.02$
		2.4	4.5	$0.9 \pm 0.06$
HW–O	0.0048	1.3	2.4	$0.6 \pm 0.08$
		2.4	4.5	$2.5 \pm 0.05$
H–OW	0.0008	1.3	2.5	$0.1 \pm 0.02$
		2.5	4.9	$0.5 \pm 0.05$
OW–H	0.0048	1.3	2.5	$0.9 \pm 0.2$
		2.5	4.9	$3.0 \pm 0.3$
H–HW	0.0016	1.5	3.2	$0.6 \pm 0.05$
		3.2	5.5	$1.0 \pm 0.06$
OW–HW	0.0016	1.2	2.4	$0.2 \pm 0.07$
		2.4	4.8	$1.4 \pm 0.2$
HW–HW	0.0552	1.5	3.1	$0.5 \pm 0.1$
cHex–cHex	0.0016	3.6	5.3	$\approx 0.8$
		5.3	7.5	$\approx 3.4$
cHex–CC	0.0048	4.0	8.2	$\approx 9.5$
CC–cHex	0.0016	4.0	8.2	$\approx 3.2$
cHex–OW	0.0008	3.0	6.2	$\approx 0.3$
		6.2	11.8	$\approx 4.9$
OW–cHex	0.0016	3.0	6.2	$\approx 0.7$
		6.2	11.8	$\approx 9.8$

interactions, respectively. Integration of the two features indicates that in the direct contact feature each cyclohexene will see  $\sim 0.3$  water molecules, while a water molecule in this environment will see  $\sim 0.7$  cyclohexene molecules. In the more distant region from 6.2 to 11.8 Å each cyclohexene molecule finds  $\sim 4.9$  water molecules while in the same distance range each water molecule would see  $\sim 9.8$  cyclohexene molecules.

A summary of the coordination numbers corresponding to the molecular centers functions is given in Table 3.

**C. Alcohol–Alcohol, Alcohol–Water, and Water–Water Hydrogen Bonding.** Figure 3 shows the site–site partial structure factors related to hydrogen bonding interactions between the alcohol molecules and the water molecules in their various combinations, namely,  $g_{O-O}(r)$ ,  $g_{O-H}(r)$ ,  $g_{H-H}(r)$ ,  $g_{O-OW}(r)$ ,  $g_{O-HW}(r)$ ,  $g_{H-OW}(r)$ ,  $g_{H-HW}(r)$ ,  $g_{OW-HW}(r)$ , and  $g_{HW-HW}(r)$ . All these functions display strong features in the distance range from  $\sim 1.5$  to  $\sim 4$  Å indicative of the importance that hydrogen bonding interactions play in the underlying structure of the trimolecular mixture. Coordination number information relating to these partial distribution functions is given in Table 3.

Panels A, B, and C of Figure 3 show the pair distribution functions relating to interalcohol hydrogen bonding via the hydroxyl group oxygen (O) and hydrogen (H) sites. The first peaks in  $g_{O-O}(r)$ ,  $g_{O-H}(r)$ , and  $g_{H-H}(r)$  come at 2.7, 1.8, and 2.4 Å, respectively, and have integrated coordination numbers of  $1.6 \pm 0.1$ ,  $0.5 \pm 0.05$ , and  $1.7 \pm 0.1$  for oxygen about

oxygen, hydrogen about oxygen, and hydrogen about hydrogen. The integrated areas of the second peaks in these three functions lead to coordination numbers of  $2.0 \pm 0.1$ ,  $1.8 \pm 0.1$ , and  $1.7 \pm 0.1$ .

Panels D, E, F, and G of Figure 3 show the pair distribution functions relating to alcohol hydroxyl group–water hydrogen bonding. As expected due to the similar chemical nature of the alcohol hydroxyl group and the water molecule, the position of the first peak in each of these functions is highly comparable to those determined for the comparable alcohol–alcohol hydroxyl group correlations and as we shall see, the water–water hydrogen bonding interactions, i.e., 2.7, 1.7, 1.8, and 2.4 Å respectively for  $g_{O-OW}(r)$ ,  $g_{O-HW}(r)$ ,  $g_{H-OW}(r)$ , and  $g_{H-HW}(r)$ . The coordination numbers associated with the number of water oxygen and hydrogen atoms around the hydroxyl group's oxygen and hydrogen sites in the distance range corresponding to these first direct hydrogen bonding correlations are  $0.4 \pm 0.04$ ,  $0.2 \pm 0.02$ ,  $0.1 \pm 0.02$ , and  $0.6 \pm 0.05$ . These numbers are small due to the dilute nature of the water in the mixture; however, performing the calculation to evaluate how many alcohol hydroxyl group oxygen atoms are directly coordinated to a water molecule oxygen atom shows that on average  $2.3 \pm 0.2$  alcohol hydroxyl groups will be found in the range 2.3 to 3.8 Å around a water molecule in the system.

Figure 3H,I and Figure 2B provide us with the pair distribution information relating to water–water interactions. As mentioned in the earlier discussion of the water–water molecular centers function (Figure 2B), these distribution functions are quite different in form to those found for the pure liquid, yet they retain the key first neighbor distance correlations characteristic of water–water hydrogen bonding: 1.7 and 2.3 Å for  $g_{OW-HW}(r)$  and  $g_{HW-HW}(r)$ , respectively. The integrated coordination numbers immediately tell us, however, that there is insufficient water in the system to generate an extended hydrogen bonded water network. In this trimolecular mixture each water oxygen atom is on average hydrogen bonded to  $0.2 \pm 0.07$  water hydrogen atoms, where in the pure liquid  $\sim 2$  atoms would be expected in the distance range defined by the first peak in  $g_{OW-HW}(r)$ .

**D. Spatial Density Functions and the 3-Dimensional Structure of the Solution.** Detailed insight into the near-neighbor 3-dimensional structure of this complex molecular mixture can be obtained from an examination of the spatial density functions (SDFs),  $g_c(r, \Omega)$ ,<sup>26</sup> calculated for each of the nine pairwise combinations of the three molecular components. These functions represent a 3-dimensional map of the density of molecular centers of one molecular species around another as a function of radial distance,  $r$ , and orientation  $\Omega = (\theta, \phi)$ , relative to the molecule placed at the origin and averaged over all orientations of the neighboring molecule.<sup>27</sup> The nine near-neighbor SDFs for cyclohexene, *tert*-butyl alcohol, and water are shown in Figure 4.

First, considering the like-molecule interactions in the solution, Figure 4A illustrates the most favorable direct interaction geometries from cyclohexene molecules in the mixture. The direct contact interactions appear to consist of two main types characterized by the large continuous lobes around the CH<sub>2</sub> groups in the ring showing a general tendency to pack these nonpolar CH<sub>2</sub> groups together and four distinct orientationally localized lobes around the H–C=C–H linkage indicative of an additional tendency to pack the C=C linkages of neighboring molecules when appropriate configurations occur in the liquid. Figure 4E highlights the most favorable alcohol–alcohol direct contact geometries and illustrates two types of dominant

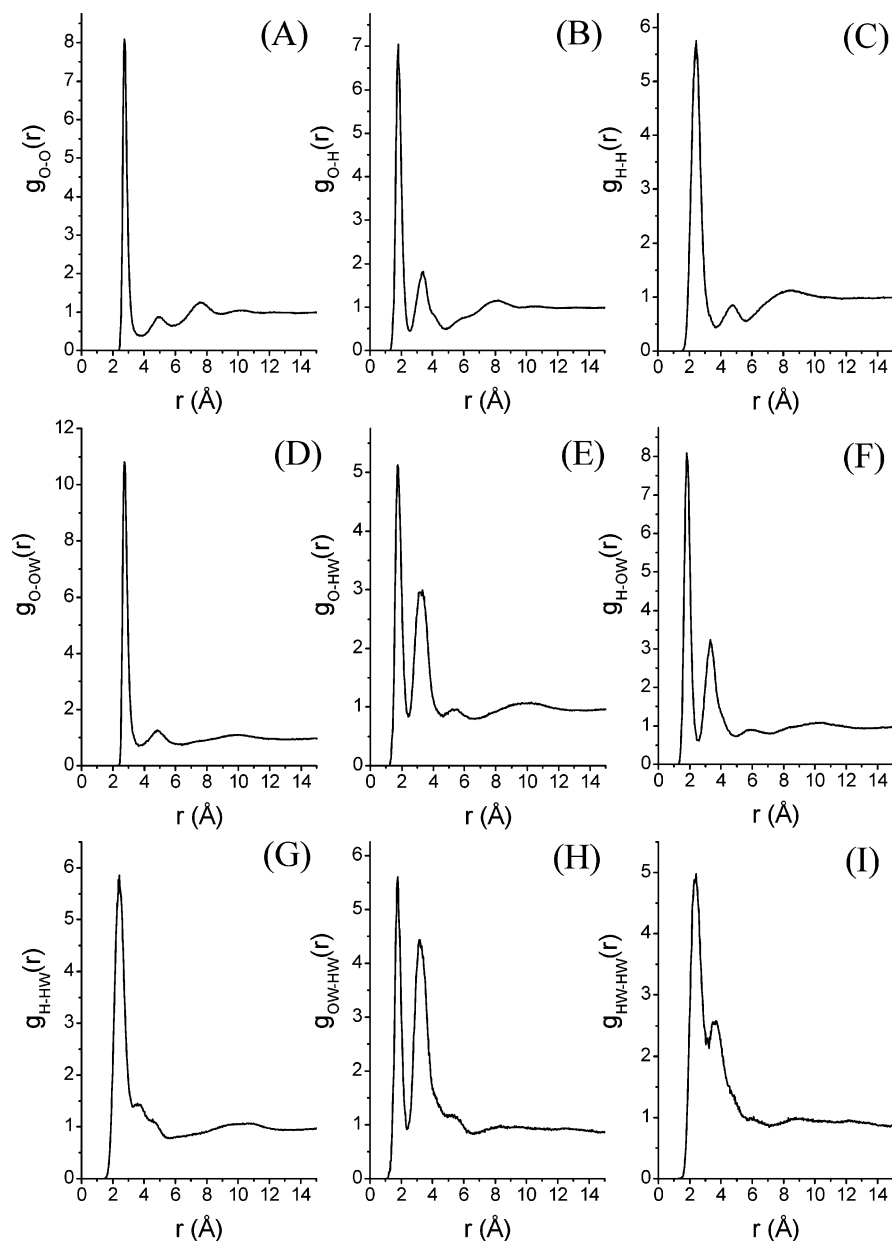


**Figure 3.** EPSR refinement derived alcohol and water atomic site–site partial distribution functions relevant to the hydrogen bonding interactions in the trimolecular mixture of cyclohexene, *tert*-butyl alcohol, and water: (A) alcohol hydroxyl group oxygen to alcohol hydroxyl group oxygen (O–O), (B) alcohol hydroxyl group oxygen to alcohol hydroxyl group hydrogen (O–H), (C) alcohol hydroxyl group hydrogen to alcohol hydroxyl group hydrogen (H–H), (D) alcohol hydroxyl group oxygen to water oxygen (O–OW), (E) alcohol hydroxyl group oxygen to water hydrogen (O–HW), (F) alcohol hydroxyl group hydrogen to water oxygen (H–OW), (G) alcohol hydroxyl group hydrogen to water hydrogen (H–HW), (H) water oxygen to water hydrogen (OW–HW), and (I) water hydrogen to water hydrogen (HW–HW).

interaction between the polar hydroxyl groups and between the nonpolar methyl group regions. The former is characterized by the trefoil saucer shaped lobe of intensity below the hydroxyl group of the central molecule, and the latter by the three lobes rising up around the methyl group region. Figure 4I shows the classic near-tetrahedral interaction geometry of the water molecule<sup>28</sup> indicating that even in this dilute solution, at least from the viewpoint of water concentration, the most favorable interactions between water molecules are still dominated by the hydrogen bonding interactions that are characteristic of the bulk solvent state. The two lobes above the hydrogen atoms on the central molecule are characteristic of the location of water molecules accepting hydrogen bonds from the central molecule, and the diffuse lobe below the central water molecule's oxygen atom indicates the most likely location of neighboring water molecules that donate hydrogen bonds to the central molecule.

Panels B and D of Figure 4 tell us about the intermolecular interactions between cyclohexene and *tert*-butyl alcohol molecules. Figure 4B shows us that there is a distinct preference for the *tert*-butyl alcohol molecules to favor localization around the C=C double bond linkage of the cyclohexene ring, while Figure 4D tells us that these molecular contacts most favorably involve the nonpolar methyl groups of the alcohol molecule.

Panels C and 4G of Figure 4 show the spatial nature of the cyclohexene–water interactions. Cyclohexene is very nonpolar and generally considered insoluble in water and the interactions between these two molecules would generally be expected to be dominated by hydrophobic hydration geometries, and this is what is clearly found. Figure 4C indicates that when water molecules interact with cyclohexene molecules they have a preference to solvate the plane of the ring structure while Figure 4G shows us very clearly that the water molecule is aligned

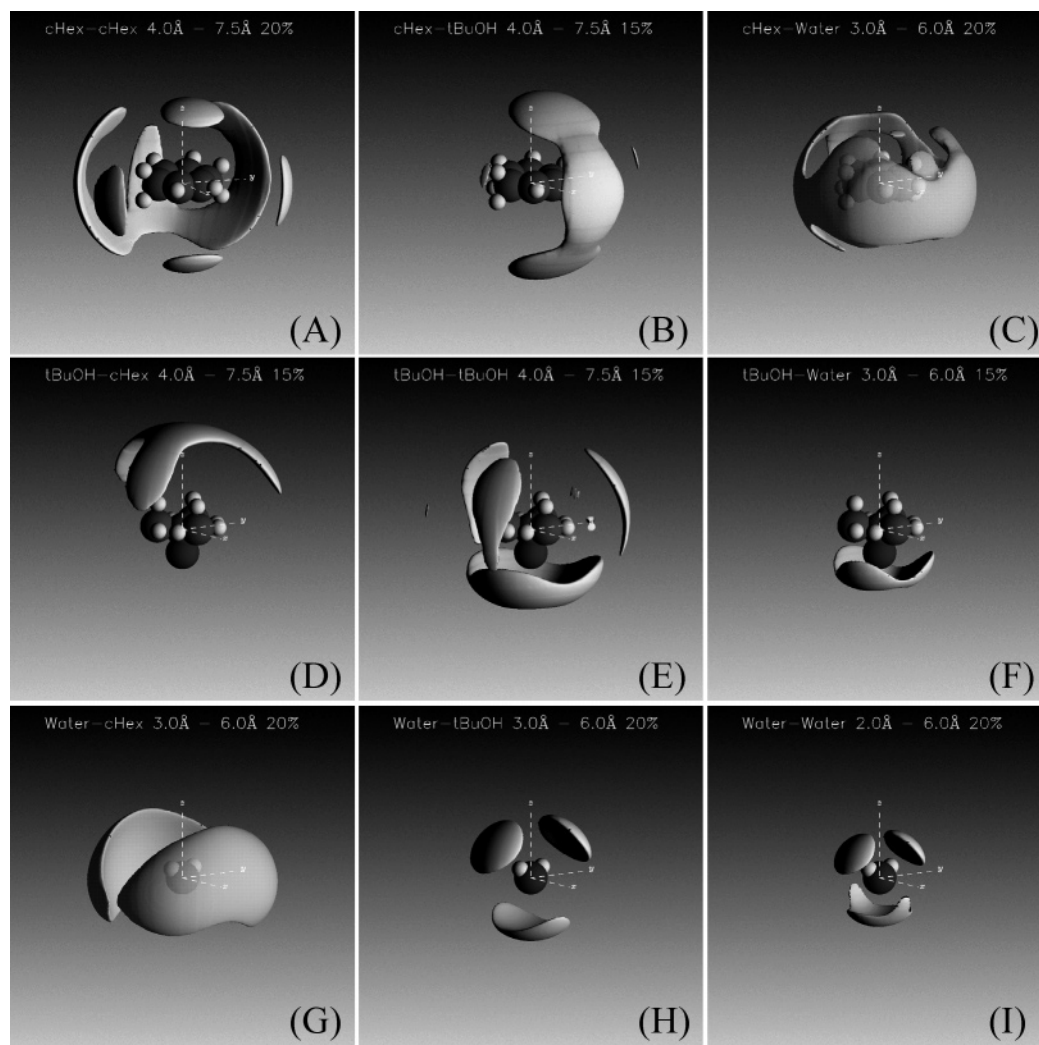


**Figure 4.** The spatial density functions (SDFs) that characterize the near neighbor molecular interactions between the three molecular species in solution: cyclohexene, *tert*-butyl alcohol, and water. This function represents a three-dimensional map of the density of the center of one molecular species about another as a function of radial distance ( $r$ ) and relative orientation ( $\Omega = \theta, \phi$ ) to the molecular species placed at the origin of the plot. In turn, the panels show (A) the SDF showing the regions where the most probable 20% of the total number of cyclohexene molecules would be found around another cyclohexene molecule in the distance range from 4.0 to 7.5 Å, (B) the SDF showing the locations corresponding to finding the most probable 15% of *tert*-butyl alcohol molecules around a cyclohexene molecule in the distance range from 4.0 to 7.5 Å, (C) the SDF showing the regions where the most probable 20% of water molecules would be located around a cyclohexene molecule in the distance range from 3.0 to 6.0 Å, (D) the SDF showing the most regions favored by the most probable 15% of cyclohexene molecules found around a *tert*-butyl alcohol molecule in the distance range from 4.0 to 7.5 Å, (E) the *tert*-butyl alcohol–*tert*-butyl alcohol SDF showing the top 15% correlation regions in the distance range from 4.0 to 7.5 Å, (F) the *tert*-butyl alcohol–water SDF showing the most likely location of finding the top 15% of water molecules around the alcohol molecule in the distance range from 3.0 to 6.0 Å, (G) the SDF showing the most regions defined by finding the most probable 20% of cyclohexene molecules around a water molecule in the distance range from 3.0 to 6.0 Å, (H) the alcohol around water SDF showing the top 20% region for finding a *tert*-butyl alcohol molecule in the distance range from 3.0 to 6.0 Å, and (I) the top 20% water–water SDF in the distance range from 2.0 to 6.0 Å.

tangentially to the cyclohexene molecule in the classic hydrophobic hydration geometry where the molecule's H–O–H plane is exposed to the nonpolar surface.<sup>1</sup>

Panels F and H of Figure 4 illustrate the most favorable direct interaction between the *tert*-butyl alcohol and water molecules. As expected, Figure 4F shows that the interactions are dominated by hydrogen bonding between the alcohol molecule's hydroxyl group and the water molecules, where Figure 4H shows us that the alcohol molecule adopts one of the close to tetrahedrally distributed hydrogen bonding sites around the water molecule.

## VI. Discussion

The presented results provide us with a detailed insight into the type and balance of the intermolecular interactions that exist in this complex three-component molecular mixture. An inter-

esting and important comparison that can now be made is with the results obtained from detailed studies of binary systems, in particular concentrated 6:1 *tert*-butyl alcohol–water solutions.<sup>8,29</sup> This comparison will allow us to determine the structural effects that the addition of cyclohexene to such a solution will have.

The principal finding of the studies on the binary 6:1 alcohol–water mixture was the development of microscopic separation of the two molecular components and the creation of small pockets of water molecules, strongly associated with the hydroxyl regions of the major alcohol component. The creation of these small regions of clustered water had a marked effect on the interactions that normally take place between the alcohol molecules in the absence of water. The presence of the water clusters effectively suppressed direct alcohol–alcohol hydrogen bonding to a level approximately 50% of that found in the pure



system,<sup>5,6</sup> driven by the preference for the alcohol molecules to solvate the water pockets instead of hydrogen bond to each other. It is immediately of note therefore that the addition of cyclohexene to the 6:1 *tert*-butyl alcohol–water solution restores the level of hydrogen bonding between the alcohol molecules to a level equivalent to, if not marginally greater than, the level that would be expected in the pure system.

The restoration of the degree of interalcohol hydrogen bonding has a marked effect on the microscopic segregation of the alcohol and water components. In the three-component system, there appears to be no obvious sign of segregation of the various components into small regions of higher like-molecule density. This reduction in the self-association of water molecules in the three-component solution can be seen in a comparison of the water–water molecular centers function  $g_{\text{ow}}(r)$  of the binary *tert*-butyl alcohol–water solution. In the binary solution each water molecule has on average  $1.5 \pm 0.4$  water molecules in the distance range out to  $5.5 \text{ \AA}$ ,<sup>29</sup> whereas in the three-component mixture this is reduced to  $1.2 \pm 0.2$  water molecules in the region out to a radial distance of  $5.9 \text{ \AA}$ . The addition of cyclohexene to the system has thus effectively produced a more homogeneous molecular mixture. The addition of the nonpolar cyclohexene molecule to the alcohol–water solution allows for better packing of the nonpolar methyl groups of the dominant alcohol mixture component that then permits the restoration of a significant quantity of alcohol–alcohol hydrogen bonding. This effect looks to be due to the similar sizes of the cyclohexene molecules and *tert*-butyl alcohol molecules and the fact that the nonpolar character of the alkene strongly drives its affinity for association with the nonpolar methyl groups of the alcohol. This effect counterbalances the natural trend for the water molecules to cluster and drive the association of the alcohol molecules through hydrophilic solvation of the small pockets of water molecules.<sup>29</sup>

The nonpolar character of the cyclohexene molecules that drives their natural affinity for the methyl groups of the alcohol molecules is also seen to drive their separation from the water component in the mixture. This is quantified by the very low near-neighbor cHexene–OW coordination numbers and based on the simple assumption that the radius of the cyclohexene molecule is  $\sim 3.5 \text{ \AA}$ . Though alkene–water interactions are kept to a minimum in this trimolecular mixture, where they do occur, the molecular contacts take on the structural characteristics of standard hydrophobic hydration, i.e., tangential water orientation relative to the hydrophobic molecular surface. The water molecules, though not clustering significantly in the three-component system, retain their preference for localization close to the alcohol molecule hydroxyl groups. Considering the average water oxygen environment in the distance range from  $2.3$  to  $3.8 \text{ \AA}$  one finds on average  $0.5 \pm 0.1$  other water oxygen atoms and  $2.3 \pm 0.2$  alcohol hydroxyl group oxygen atoms placing a total of  $\sim 3$  hydrogen bond capable groups within the appropriate range for hydrogen bonding. In pure water and water-rich alcohol–water solutions just over 4 hydrogen bond capable groups would be found in this region.

The finding that in the trimolecular mixture the water hydrogen bonding capacity is not fully satisfied is analogous to the situation found for water in the simple 6:1 alcohol–water solution, where similar levels of hydrogen bonding were observed.<sup>8</sup> The principal impact that the addition of cyclohexene to the system seems to have had on the local water molecule environment is to disperse the clustering without significantly impacting the degree of hydrogen bonding that each molecule can achieve, effectively enhancing the amount of water–alcohol

hydrogen bonding and reducing the amount of water–water hydrogen bonding.

## VII. Conclusions

The results obtained for the intermolecular structure in the trimolecular liquid of cyclohexene, *tert*-butyl alcohol, and water present a picture of a well-mixed solution where the competing contributions of the nonpolar cyclohexene molecules and the polar water molecules are balanced within the matrix of the bulk *tert*-butyl alcohol solvent, where “balanced” relates to the level of interalcohol molecule hydrogen bonding compared to the pure alcohol reference state. The comparable molecular sizes of cyclohexene and *tert*-butyl alcohol and their largely complementary nature result in a well-ordered solution on the length scale of a few molecular diameters with the much smaller water molecules fitting into the regions around the alcohol molecules polar hydroxyl groups. In this environment the water molecules can maintain reasonable quantities of hydrogen bonding interactions despite the relatively low proportion of water in the system.

The improved homogeneity of the mixture when compared with that of the binary 6:1 *tert*-butyl alcohol–water system is likely to have a marked effect on the solution’s capacity to act as a host medium for chemical reaction processes. The solution is considerably less biphasic than the binary alcohol–water system and does not appear to support microclustering of the water molecules around the alcohol hydroxyl groups though water-like hydrogen bonding regions still exist through a combination of interactions between the alcohol hydroxyl groups and dispersed water molecules.

## References and Notes

- (1) Bowron, D. T. *Philos. Trans. R. Soc. London, Ser. B* **2004**, 359, 1167.
- (2) Enderby, J. E.; Neilson, G. W. In *Water: A Comprehensive Treatise*, Franks, F., Ed.; Plenum: New York, 1979; Vol. 6, pp 1–46.
- (3) Finney, J. L.; Soper, A. K. *Chem. Soc. Rev.* **1994**, 23, 1.
- (4) Franks, F.; Desnoyers, J. E. *Water Sci. Rev.* **1985**, 1, 171.
- (5) Bowron, D. T.; Finney, J. L.; Soper, A. K. *Mol. Phys.* **1998**, 93, 531.
- (6) Bowron, D. T.; Finney, J. L.; Soper, A. K. *Mol. Phys.* **1998**, 94, 249.
- (7) Bowron, D. T.; Finney, J. L.; Soper, A. K. *J. Phys. Chem. B* **1998**, 102, 3551.
- (8) Bowron, D. T.; Díaz Moreno, S. J. *Chem. Phys.* **2002**, 117, 3753.
- (9) Finney, J. L.; Bowron, D. T.; Daniel, R. M.; Timmins, P. A.; Roberts, M. A. *Biophys. Chem.* **2003**, 105, 391.
- (10) Dixit, S.; Crain, J.; Poon, W. C. K.; Soper, A. K.; Finney, J. L. *Nature* **2002**, 416, 829.
- (11) Dixit, S.; Crain, J.; Poon, W. C. K. *J. Phys.: Condens. Matter* **2000**, L323, 12.
- (12) Sato, T.; Buchner, R. J. *Chem. Phys.* **2003**, 119, 10789.
- (13) Kolb, H. C.; VanNieuwenhze, S.; Sharpless, K. B. *Chem. Rev.* **1994**, 94, 2483.
- (14) Keen, D. A. *J. Appl. Crystallogr.* **2000**, 34, 172.
- (15) Soper, A. K. Rutherford Appleton Laboratory, private communication.
- (16) Soper, A. K.; Howells, W. S.; Hannon, A. C. ATLAS-Analysis of Time-of-Flight Diffraction Data from Liquid and Amorphous Samples; Rutherford Appleton Laboratory Report RAL 89-046, 1989.
- (17) Soper, A. K.; Luzar, A. *J. Phys. Chem. B* **1992**, 97, 1320.
- (18) Soper, A. K. *Chem. Phys.* **1996**, 202, 296.
- (19) Soper, A. K. In *Local Structure from Diffraction*; Billinge, S. J. L., Thorpe, M. F., Eds.; Plenum: New York, 1998; 59–83.
- (20) Soper, A. K. *Mol. Phys.* **2001**, 99, 1503.
- (21) Allen, M. P.; Tildesley, D. J. *Computer Simulation of Liquids*; Oxford University Press: Oxford, UK, 1987.



- (22) Soper, A. K. Partial Structure Factors from disordered materials diffraction data: an approach using Empirical Potential Structure Refinement. *Phys. Rev. B* **2005**, in press.
- (23) Soper, A. K. *Chem. Phys.* **2000**, 258, 121.
- (24) Milano, G.; Müller-Plathe, F. *J. Phys. Chem. B* **2004**, 108, 7415.
- (25) Bowron, D. T.; Finney, J. L.; Soper, A. K. *J. Chem. Phys.* **2001**, 114, 6203.
- (26) Svishchev, I. M.; Kusalik, P. G. *J. Chem. Phys.* **2002**, 99, 3049.
- (27) Finney, J. L.; Bowron, D. T. In *From semiconductors to proteins: beyond the average structure*; Billinge, S. J. L., Thorpe, M. F., Eds.; Kluwer: Dordrecht, The Netherlands, 2002; pp 219–244.
- (28) Soper, A. K. *J. Chem. Phys.* **1994**, 101, 6888.
- (29) Bowron, D. T.; Díaz Moreno, S. *J. Phys.: Condens. Matter* **2003**, 15, S121.